



# Past, present and future rainfall erosivity in central Europe based on convection-permitting climate simulations

Magdalena Uber<sup>1</sup>, Michael Haller<sup>2</sup>, Christoph Brendel<sup>3</sup>, Gudrun Hillebrand<sup>1</sup>, and Thomas Hoffmann<sup>1</sup>

<sup>1</sup>Department of Fluvial Morphology, Sediment Dynamics and Management,  
Federal Institute of Hydrology, 56068 Koblenz, Germany

<sup>2</sup>Climate and Environment Consultancy, Deutscher Wetterdienst, 63067 Offenbach am Main, Germany

<sup>3</sup>Hydrometeorology, Deutscher Wetterdienst, 63067 Offenbach am Main, Germany

**Correspondence:** Magdalena Uber (uber@bafg.de)

Received: 5 May 2023 – Discussion started: 11 May 2023

Revised: 3 November 2023 – Accepted: 7 November 2023 – Published: 5 January 2024

**Abstract.** Heavy rainfall is the main driver of soil erosion by water, which is a threat to soil and water resources across the globe. As a consequence of climate change, precipitation – especially extreme precipitation – is increasing in a warmer world, leading to an increase in rainfall erosivity. However, conventional global climate models struggle to represent extreme rain events and cannot provide precipitation data at the high spatiotemporal resolution that is needed for an accurate estimation of future rainfall erosivity. Convection-permitting simulations (CPSs), on the other hand, provide high-resolution precipitation data and a better representation of extreme rain events, but they are mostly limited to relatively small spatial extents and short time periods. Here, we present, for the first time, rainfall erosivity in a large modeling domain such as central Europe based on high-resolution CPS climate data generated with the regional climate model COSMO-CLM using the Representative Concentration Pathway 8.5 (RCP8.5) emission scenario. We calculated rainfall erosivity for the past (1971–2000), present (2001–2019), near future (2031–2060) and far future (2071–2100). Our results showed that future increases in rainfall erosivity in central Europe can be up to 84 % in the region’s river basins. These increases are much higher than previously estimated based on regression with mean annual precipitation. We conclude that despite remaining limitations, CPSs have an enormous and currently unexploited potential for climate impact studies on soil erosion. Thus, the soil erosion modeling community should closely follow the recent and future advances in climate modeling to take advantage of new CPSs for climate impact studies.

## 1 Introduction

Soil erosion by water is one of the main threats to soils worldwide (Amundson et al., 2015; Panagos et al., 2015a). It causes severe ecological and socioeconomic problems such as ecosystem degradation (Bilotta and Brazier, 2008; Orgiazzi and Panagos, 2018; Mueller et al., 2020; Stefanidis et al., 2022), loss of fertile topsoil on agricultural land (Pimentel et al., 1995; Zhao et al., 2013; Sartori et al., 2019), channel and reservoir siltation (Wisser et al., 2013; Kondolf et al., 2014), and nutrient and contaminant transport to waterbodies (Owens et al., 2005; Ciszewski and Grygar, 2016). Heavy rainfall is the main driving force of soil erosion by water. It acts via the detachment of soil particles by raindrop impact or shear forces of overland flow and subsequent transport of soil particles with overland flow. Rainfall erosivity was first quantified in the 1950s and can be defined as “the capability of rainfall to cause soil loss from hillslopes by water” (Nearing et al., 2017). It is most commonly expressed as the *R* factor of the Universal Soil Loss Equation (USLE; Wischmeier and Smith, 1978) and its revised versions RUSLE (Renard et al., 1993) and RUSLE2 (USDA Agricultural Research Service, 2008). The USLE, its different versions and models based on the USLE are the most widely used soil erosion models (Borrelli et al., 2021). The USLE calculates average annual soil loss at a site from rainfall erosivity, soil erodibility, topography, crop management and control practices.

Rainfall erosivity is governed by rainfall kinetic energy, which itself depends on raindrop numbers, sizes and fall ve-

localities (e.g., Laws and Parsons, 1943; Wilken et al., 2018). As drop size distributions and fall velocity distributions are usually not available for long periods of time and large study sites, rainfall intensity is usually used as a proxy. Numerous kinetic energy–rainfall intensity relations exist in the literature and are used in soil erosion modeling (Van Dijk et al., 2002; Wilken et al., 2018; Brychta et al., 2022). Site-specific rainfall erosivity expressed as the USLE  $R$  factor is commonly calculated from long-lasting precipitation records from rain gauges. The suitability of  $R$ -factor equations to represent rainfall erosivity depends strongly on the temporal resolution of the underlying precipitation data time series.  $R$  factors decrease with decreasing resolution of the precipitation data because intensity peaks are reduced when precipitation is aggregated over longer time spans (Fischer et al., 2018). When high-resolution precipitation data are only available at a few locations or for limited time periods but low-resolution data (daily–annual) are available elsewhere (e.g., denser rain gauge networks, past reconstructions or future projections), so-called low-resolution approaches can be applied (Brychta et al., 2022). These approaches are based on empirical relations between rainfall erosivity calculated from high-resolution data and lower-resolution rainfall amounts (usually monthly, seasonal or annual totals). Application of these approaches to calculate future changes in rainfall erosivity is not permitted if the frequency distribution of rainfall events changes, as expected under climate change.

Erosion modeling usually requires contiguous data of rainfall erosivity which is highly variable in space (Auerswald et al., 2019a). This spatial variability is usually not represented by rain gauge networks, so spatially interpolated raster data are necessary. Gauge-adjusted radar rainfall data have a high potential for the estimation of highly resolved and contiguous rainfall erosivity maps (Fischer et al., 2018; Risal et al., 2018; Auerswald et al., 2019a; Kreklow et al., 2020). Where ground-based radar data are not available, satellite-based gridded precipitation data sets can also be used to generate contiguous maps (Vrieling et al., 2010; Teng et al., 2017; Phinzi and Ngetar, 2019).

Globally, precipitation is increasing due to an increase in atmospheric water vapor in warmer air (e.g., Allan et al., 2020; Fowler et al., 2021). For central Europe, a net increase in total precipitation is projected with a decrease in summer and an increase in winter (Brienen et al., 2020; Jacob et al., 2014). Furthermore, warming and higher atmospheric moisture fluxes lead to an intensification of the water cycle, causing an increase in the intensity and frequency of extreme precipitation, globally as well as in central Europe (Allan et al., 2020; Brienen et al., 2020; Fowler et al., 2021). Strong increases in extreme precipitation are due to the fact that the share of convective precipitation in total precipitation is increasing (Berg et al., 2013). Trends of an increase in the frequency and intensity of extreme precipitation have been observed since the beginning of the 20th century (Groisman et al., 2005; Alexander et al., 2006; Arnone et al., 2013; Kendon

et al., 2014; Fischer and Knutti, 2016) and are expected to continue in the future (Allen and Ingram, 2002; Kharin et al., 2013; Scoccimarro et al., 2013; Westra et al., 2013, 2014; Kendon et al., 2017; Fowler et al., 2021). Thus, rainfall erosivity and soil erosion have also been observed to increase and are expected to increase further (Nearing et al., 2004; Mueller and Pfister, 2011; Hanel et al., 2016a; Panagos et al., 2017, 2022; Auerswald et al., 2019a, b; Borrelli et al., 2020).

For climate impact studies on soil erosion, a common limitation is the lack of reliable high-resolution precipitation data for the future (Eekhout and De Vente, 2020). Projections of future precipitation from regional climate models in Europe are typically available at a temporal resolution of 1 d and a spatial resolution of  $0.11^\circ$  (approx. 12 km) (e.g., Jacob et al., 2014). Thus, low-resolution approaches based on regression models that estimate future  $R$  factors from monthly or annual precipitation are commonly applied (Eekhout and De Vente, 2020). Out of 68 climate impact assessment studies reviewed by Eekhout and De Vente (2020), only 4 used sub-daily precipitation data. In the review of 3030 soil erosion modeling studies by Borrelli et al. (2021), 196 were identified to have the aim to model “climate change” or “land use change and climate change” impacts. Only 11 out of the 196 studies are quoted to use sub-daily precipitation data. The few studies that use hourly or sub-hourly future precipitation data mostly use either statistical downscaling of lower-resolution data (Routschek et al., 2015; Wang et al., 2018) or artificially generated precipitation time series (e.g., Coulthard et al., 2012; Simonneaux et al., 2015). Strictly speaking, regression-based models applying monthly or annual precipitation are only valid for the time period for which these models are calibrated and lead to underestimations of the rainfall erosivity if extreme precipitation events increase with time, as suggested by many climate change scenarios.

Only recently, the development of convection-permitting simulations (CPSs) has offered the possibility to model rain erosivity considering the effects of a changing frequency of heavy precipitation that predominantly drives future soil erosion. Thus, CPSs have an enormous and currently unexploited potential for the calculation of future rainfall erosivity. CPSs are performed with regional climate models (RCMs) at a high spatial resolution (usually  $\leq 4$  km). Due to the coarse resolution of conventional climate simulations, deep convection has to be parameterized as a sub-grid-scale process, which leads to deficits in the realistic simulation of precipitation. This parameterization is switched off in the model setup of a CPS (Lucas-Picher et al., 2021), allowing the model to simulate the precipitation explicitly in each grid cell. A good representation of deep convection is crucial, as it is the main source of precipitation in many parts of the world and is especially important because it often generates extreme precipitation (Prein et al., 2015). As the grid size of most CPSs still ranges between 2 and 4 km, large deep convection cells are explicitly simulated, while smaller shallow convection still needs to be simulated using a parameteriza-

tion. Despite this shortcoming, CPSs provide an improved representation of extreme precipitation compared with climate models with parameterized deep convection. This is due to several improvements: the diurnal cycle is strongly improved (Ban et al., 2014; Prein et al., 2015), the return periods of extreme precipitation are better represented (Rybka et al., 2022) and added value diagnostics have been applied for the comparison to coarse climate model data (Raffa et al., 2021). However, CPSs also show some limitations: simulations at the kilometer scale for regional domains are still time-consuming and they need a considerable amount of computing power. Compromises have to be made: either the covered time period is shortened or the model domain is restricted to the region of interest. Until some years ago, only single CPSs were performed, covering only one future scenario. Thus, given the novelty of CPSs, model ensembles are not yet available for regional model domains, for the length of the time series needed for the robust estimation of rainfall erosivity ( $\sim 20$  years) or for several emission scenarios. Lately, first-of-their-kind CPS ensembles have been created through combined efforts in the CPS community (Coppola et al., 2020; Ban et al., 2021). Even though these ensemble simulations do not yet cover the long time periods needed for the estimation of rainfall erosivity, these flagship studies show promising results which suggest that ensembles of CPSs will be available for climate impact studies including studies on soil erosion in the future.

The COSMO-CLM is a regional climate model that is used on horizontal scales from 1 to 50 km (Rockel et al., 2008). It is the climate version of the former operational forecast model of the Consortium for Small-scale Modeling (COSMO) of the German meteorological service (Deutscher Wetterdienst, DWD) and other European partners. COSMO-CLM is jointly maintained and developed by the climate limited-area modeling (CLM) community (CLM-Community) but will soon be gradually replaced by the newly developed regional climate model ICON-CLM (Pham et al., 2021). In the framework of the BMDV Expertennetzwerk project, CPSs have been performed with COSMO-CLM. Three time periods, including one historical period (1971–2000, called CPS-hist) and two future periods (CPS-scen, near future: 2031–2060; far future, 2071–2100), were simulated by dynamically downscaling from global model data. Additionally, evaluation simulations were conducted with reanalysis data forcing for the 1971–2019 time period (CPS-eval). The data are published and usable for manifold analyses and impact model studies (Brienen et al., 2022; Haller et al., 2022a, b).

The improved representation of extreme precipitation in CPSs compared with conventional convection-parameterized climate models as well as the high spatiotemporal resolution of CPSs is of great benefit for climate impact studies in soil erosion modeling (Chapman et al., 2021). Using CPSs with a high temporal resolution facilitates the direct calculation of the  $R$  factor and avoids the application of regression equa-

tions between the  $R$  factor and annual precipitation, which are established for past climates but may not be valid for a future climate with a different precipitation frequency and magnitude. To our knowledge, to date, only one study (Chapman et al., 2021) has assessed the impact of climate change on soil erosion using a convection-permitting climate model. They used 15 min precipitation data from the pan-African Climate Predictions for Africa (CP4A) model to calculate rainfall erosivity in Tanzania and Malawi for 8 years in the past and 8 years in the future. Their results suggested that convection-parameterized regional and global climate models might underestimate future rainfall erosivity, while CPSs represent observed storm characteristics better. Nonetheless, there are remaining limitations of CPSs that hinder their use in soil erosion modeling:

- i. *The limited spatial extent of most CPSs.* While regional and global convection-parameterized simulations cover the entire globe, CPSs are currently only available for limited areas in most regions of the world (e.g., central Europe) due to constraining factors like computing power.
- ii. *The relatively short periods of time covered by CPSs.* Because of the high interannual variability in rainfall erosivity, long time series are required for robust estimates of long-term  $R$  factors. Wischmeier and Smith (1958) give a minimum of 20 years.
- iii. *The lack of model ensembles.* While ensembles of regional or global climate models give more robust estimates of the future climate than single ensemble members, development of CPS ensembles has only recently started.

Covering an area of approx.  $1.6 \times 10^6$  km<sup>2</sup> on land and 109 years in total, the CPSs performed with COSMO-CLM by the DWD overcome limitations (i) and (ii) for the first time and are, thus, a valuable source of precipitation data for the estimation of rainfall erosivity in central Europe.

In this study, we calculated rainfall erosivity in central Europe, expressed as the USLE  $R$  factor, for the past (1971–2000), present (2001–2019), near future (2031–2060) and far future (2071–2100) from convection-permitting climate model output using the Representative Concentration Pathway 8.5 (RCP8.5) emission scenario. We assessed changes in rainfall erosivity from the climate model output for a historical and future time period. Finally, we discuss the potential and limitations of using CPSs for the calculation of rainfall erosivity. The main remaining limitation is the fact that ensembles of CPSs that cover at least 20 years, as needed for robust rainfall erosivity estimations, do not currently exist. As a consequence, the uncertainty due to the choice of the model and the emission scenario cannot be assessed. To address this problem, we compare our results to those obtained from an ensemble of conventional RCMs as well as to results

from the literature. To our knowledge, this is the first test case that applies CPSs to the calculation of rainfall erosivity covering national spatial scales and time series with a length in the order of 30 years.

## 2 Material and methods

### 2.1 COSMO-CLM

Convection-permitting simulations were conducted using the non-hydrostatic COSMO-CLM RCM. It shares almost all relevant modules with the COSMO weather forecast model (Doms et al., 2001), which has been the operational weather forecast model of the DWD for more than a decade, before it was replaced by the ICON model (Giorgetta et al., 2018) in recent times. COSMO-CLM, the climate version of COSMO, is optimized for long-term climate runs of more than 15 years (Rockel et al., 2008; Sørland et al., 2021). The general COSMO characteristics (e.g., physics) are documented in Steppeler et al. (2003). COSMO-CLM is described in more detail in Böhm et al. (2006). The model is usable at different horizontal grid widths and has a typical vertical spacing of 50 layers in the troposphere and the lower stratosphere up to about 22 km. Sub-grid-scale physical processes are parameterized, as they cannot be calculated explicitly. For grid spacings of less than 4 km, the convection parameterization scheme for deep convection is turned off, while the shallow convection scheme remains turned on. In the COSMO-CLM standard parameterization for coarser grid resolutions, both parts are switched on.

The model domain of the CPS has  $415 \times 423$  grid points and is centered over Germany. It includes large parts of neighboring countries and, therefore, fully covers the contributing catchment areas of the major central European rivers, including the Rhine, Elbe, Oder and upper Danube until Bratislava (Fig. 1). The grid resolution is  $0.0275^\circ$  ( $\approx 3$  km). The model uses the standard parameterizations for turbulence and (shallow) convection as well as for time integration.

For the projection simulations, three 30-year time slices have been selected, covering the years 1971–2000 (historical, CPS-hist) as well as 2031–2060 and 2071–2100 (scenario, CPS-scen). Coupled Model Intercomparison Project Phase 5 (CMIP5) global model data from the Model for Interdisciplinary Research on Climate (MIROC5; Watanabe et al., 2010) have been dynamically downscaled, applying the RCP8.5 scenario. The downscaling has been performed using an intermediate nesting step of 12 km. This intermediate nesting was performed because it is not advised to perform direct downscaling from global models with resolutions of approx. 100 km or coarser to the very high resolution of approx. 3 km.

The CPS evaluation simulation (CPS-eval) covering the 1971–2019 time range is driven by ERA5 (Hersbach et al.,

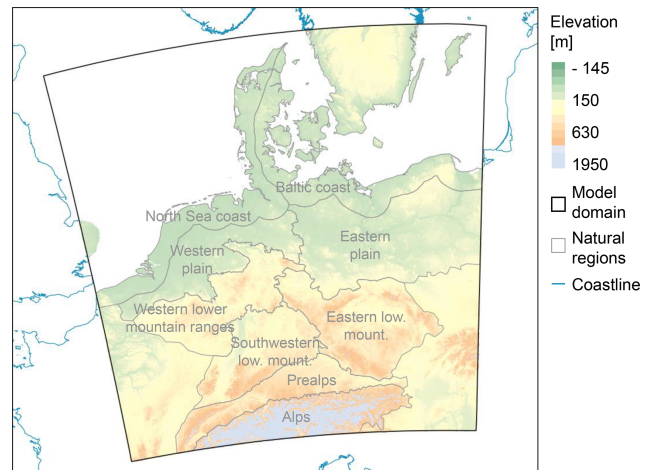


**Figure 1.** Extent of the CPS model domain. Colors show the elevation (source: EU-DEM, Copernicus Land Monitoring Service, 2016). The natural regions outlined in gray were adapted from Bundesamt für Naturschutz (2017).

2020) for the years from 1979 to 2019 and by ERA-40 reanalysis data (Uppala et al., 2005) for the years from 1971 to 1978. ERA5 and ERA-40 are reanalysis data that provide comprehensive and coherent information on essential climate variables by assimilating additional various observational data to a model grid. The model system itself remains unchanged throughout the entire time period, resulting in a consistent approach to data assimilation and various parameterizations. For the ERA-40-driven time period, we used a twofold nesting with a middle step at  $0.11^\circ$ , whereas a direct downscaling from 30 to 3 km was applied for the ERA5-driven time period. The evaluation simulation driven with reanalysis data serves as a reference for the historical simulation driven by a global climate model. It quantifies how well the historical climate can be reproduced by the historical simulation and how large the differences in specific climate variables are between both simulations. In addition, Rybka et al. (2022) used the evaluation simulation for a comparison with high-resolution observational precipitation data sets to analyze the model performance for extreme precipitation.

The COSMO-CLM CPS model output consists of hourly data for the most important variables (e.g., temperature, precipitation, humidity and wind). It is available at <https://esgf.dwd.de/projects/dwd-cps/> (last access: 10 February 2023) (Brienen et al., 2022; Haller et al., 2022a, b). The overall configuration of our simulation has been taken from a joint contribution of the CLM-Community to a CPS experimental study for central Europe (Coppola et al., 2020). The hourly precipitation data that were further processed for this study were organized in five data sets (Table 1): the projection simulations for the historical period and the near and far future (CPS-hist, CPS-scen-nf and CPS-scen-ff, respectively) as well as the evaluation simulations for the historical period

and the present (CPS-eval-hist and CPS-eval-present, respectively).

## 2.2 Calculation of rainfall erosivity

### 2.2.1 High-temporal-resolution approach

Following Wischmeier and Smith (1958, 1978) and Wischmeier (1959), the erosivity of an erosive rain event  $R_e$  ( $\text{N h}^{-1}$ ) is calculated as the product of maximum 30 min rain intensity  $I_{\max30}$  ( $\text{mm h}^{-1}$ ) and kinetic energy  $E_{\text{kin}}$  ( $\text{kJ m}^{-2}$ ) of the rain event:

$$R_e = I_{\max30} \cdot E_{\text{kin}}. \quad (1)$$

An erosive rain event is defined as having a total precipitation ( $P$ ) of at least 12.7 mm or a maximum 30 min rainfall intensity ( $I_{\max30}$ ) of at least 12.7  $\text{mm h}^{-1}$  and at least 6 h without any precipitation between two erosive rain events. We used the classical equation by Wischmeier and Smith (1978) to calculate kinetic energy based on high-resolution rainfall data. Transferred to International System of Units (SI) base units, it calculates specific kinetic energy per millimeter rain depth,  $e_{\text{kin},i}$  (in  $\text{kJ m}^{-2} \text{mm}^{-1}$ ) for every time increment during an erosive rainfall event as follows (Rogler and Schwertmann, 1981):

$$e_{\text{kin},i} = \begin{cases} 0 & \text{for } I < 0.05 \text{ mm h}^{-1} \\ (11.89 + 8.73 \cdot \log_{10} I) \cdot 10^{-3} & \text{for } 0.05 \text{ mm h}^{-1} \leq I < 76.2 \text{ mm h}^{-1} \\ 28.33 \cdot 10^{-3} & \text{for } I \geq 76.2 \text{ mm h}^{-1}. \end{cases} \quad (2)$$

To obtain  $E_{\text{kin}}$  for each event,  $e_{\text{kin},i}$  is multiplied by the rain depth of each time step and summed for the entire rain event. Annual rainfall erosivity of a specific year is obtained by summing the  $R_e$  of all erosive rain events in that year. The USLE  $R$  factor is the long-term average of annual rainfall erosivity.  $R$  factors are often given in the unit  $\text{MJ mm ha}^{-1} \text{h}^{-1} \text{a}^{-1}$ . To convert rainfall erosivity as given here in  $\text{N h}^{-1} \text{a}^{-1}$  to  $\text{MJ mm ha}^{-1} \text{h}^{-1} \text{a}^{-1}$ , it has to be multiplied by a factor of 10.

Here, we calculated annual erosivity as well as long-term average annual erosivity for each one of the 175 545 grid points and for each of the five data sets (CPS-hist, CPS-scen-nf, CPS-scen-ff, CPS-eval-hist and CPS-eval-present). We used the Climate Data Operators (CDO) command line suite (Schulzweida, 2022) and the ncdf4 library (Pierce, 2019) of the R statistical software to extract a time series of 30 years (19 years for CPS-eval-present) for each grid point and each data set and then calculated rainfall erosivity as described above. As the COSMO-CLM model output is available at a temporal resolution of 60 min, three adjustments were made as proposed by Fischer et al. (2018): (i) the rainfall intensity threshold of  $I_{\max30}$  to define an erosive rain event was lowered from 12.7 to 5.8  $\text{mm h}^{-1}$ , (ii)  $I_{\max30}$  in Eq. (1) was replaced by a maximum 60 min rainfall erosivity  $I_{\max60}$  and (iii) a temporal scaling factor of 1.9 was applied to the  $R$  factor for Germany to account for the reduction in intensity

peaks with lower-temporal-resolution data. Here, we did not apply a spatial scaling factor because it is unclear if such a modification is necessary for climate model output.

We further assessed the seasonal distribution of erosivity by calculating the erosion index for each day of the year. The erosion index gives the contribution of each day to annual erosivity (in  $\% \text{d}^{-1}$ ). The seasonal distribution of erosivity is important for soil erosion assessments, because of its interactions with seasonal changes in the crop cover. Briefly, high rainfall erosivity in months when vegetation cover is scarce (in central Europe the winter months) is more severe than high rainfall erosivity during the vegetation period (i.e., the summer months). The erosion index was calculated for each of the 175 545 grid points and each day of each year and averaged over all grid points and all 30 years in the three data sets from the projection simulations (CPS-hist, CPS-scen-nf and CPS-scen-ff). The erosion index varies strongly from one day to another and between grid points. Even averaged over all grid point and over 30 years, there still is a high remaining scatter; therefore, a 13 d moving average is used for smoothing of the curves for the three data sets.

### 2.2.2 Low-temporal-resolution approach

For comparison, we also calculated rainfall erosivity ( $R$ ) for the past (1971–2000), near future (2031–2060) and far future (2071–2100) from mean annual precipitation (MAP). Therefore, we used the empirical regression equation

$$R \left[ \text{N h}^{-1} \text{a}^{-1} \right] = 0.0788 \cdot \text{MAP}[\text{mm}] - 2.82 \quad (3)$$

from the German norm DIN 19708 (DIN-Normenausschuss Wasserwesen, 2017), which was derived from regression analysis of  $R$ -factor values calculated based on Eq. (1) and annual precipitation sums for the time period from the 1960s to the 1980s in Germany. We used the median, 15th percentile and 85th percentile of the MAP of a climate model ensemble consisting of 21 members that were run with the RCP8.5 emission scenario. The models are part of the DWD reference ensemble (<https://www.dwd.de/ref-ensemble>, last access: 20 October 2022). The low-temporal-resolution approach was used here because it allows a representation of the bandwidth of results obtained with a RCM ensemble and, thus, an estimate of model uncertainty, which is not yet possible for CPSs. Nonetheless, the main limitation, i.e., neglect of the effect of increases in heavy rain, of the approach has to be stressed again. This shortcoming is overcome by CPSs and is one of the reasons why the most recent version of DIN 19708 (DIN 19708:2022-08) recommends using Eq. (3) solely for historical observations.

**Table 1.** Information on the five data sets that were used for rainfall erosivity calculation.

Name	Temporal coverage	Driving data	Reference
CPS-eval-hist	1971–2000	ERA5, ERA-40	Brienen et al. (2022)
CPS-eval-present	2001–2019	ERA5	Brienen et al. (2022)
CPS-hist	1971–2000	MIROC5, RCP8.5	Haller et al. (2022a)
CPS-scen-nf	2031–2060	MIROC5, RCP8.5	Haller et al. (2022b)
CPS-scen-ff	2071–2100	MIROC5, RCP8.5	Haller et al. (2022b)

### 3 Results and discussion

#### 3.1 Past, present and future rainfall erosivity

##### 3.1.1 Rainfall erosivity maps

The average annual rainfall erosivity maps for the five data sets show a consistent spatial pattern (Fig. 2), which is mainly driven by topography. In all data sets, erosivity is lowest in the lowlands of the North European Plain and highest in the Alps. In the past and present, average annual erosivity in the lowlands ranges between approx. 50 and 90  $\text{N h}^{-1} \text{a}^{-1}$ . In the Alps, it ranges between 260 and 290  $\text{N h}^{-1} \text{a}^{-1}$ , and it ranges between about 90 and 130  $\text{N h}^{-1} \text{a}^{-1}$  in the lower mountain ranges. In the past, the mean of the entire modeling domain is 91  $\text{N h}^{-1} \text{a}^{-1}$  in the evaluation run (CPS-eval-hist) and 96  $\text{N h}^{-1} \text{a}^{-1}$  in the projection run (CPS-hist). It increased considerably in the future (Sect. 3.2). These maps are available on Zenodo (Uber et al., 2023) and can be used as *R*-factor maps in USLE-based soil erosion modeling.

The maps for the past calculated from the evaluation run and the projection run are very similar (Fig. 2a, c). The spatial mean of the difference between the maps is 4.9  $\text{N h}^{-1} \text{a}^{-1}$ , and the values for all grid points extracted from the two maps correlate well ( $R^2 = 0.91$ ; Fig. S1 in the Supplement).

Beyond erosion modeling, rainfall erosivity can also be regarded as an index of heavy rain that combines rainfall intensity and cumulative precipitation depth. As such, the rainfall erosivity data presented here can also provide valuable information for other hydrological applications dealing with extreme rainfall such as the assessment of (future) risks of flash floods or landslides or identifying zones that are prone to these natural risks (Fiener et al., 2013; Panagos et al., 2015b).

##### 3.1.2 Comparison to other rainfall erosivity maps

Past and present rainfall erosivity can be compared to other available rainfall erosivity maps. Figure 3 shows that rainfall erosivity calculated from the evaluation simulation for 2001–2019 agrees well with the rainfall erosivity map by Auerswald et al. (2019a). The correlation between the values of the raster cells is very good ( $R^2 = 0.94$ ) and the slope of the linear regression model is 0.98, i.e., very close to 1. Thus, there is no systematic difference between the two

data sets, and the spatial structure corresponds well to that found by Auerswald et al. (2019a). Nonetheless, there are regional differences. Rainfall erosivity in the very north of Germany and in the northwest is underestimated here when compared with Auerswald et al. (2019a), whereas it is overestimated in parts of eastern Germany, the Black Forest and in the Alps (Fig. 3b). The highest values reported here ( $> 500 \text{ N h}^{-1} \text{a}^{-1}$ ) are not found by Auerswald et al. (2019a). This might be due to the overestimation of extreme precipitation in COSMO-CLM (Sect. 3.3; Rybka et al., 2022). Compared with the other rainfall erosivity maps for Europe (Panagos et al., 2015b), the Czech Republic (Hanel et al., 2016b) and Austria (Johannsen et al., 2022), our values are, on average, about 2 times higher than those of the other authors. Nonetheless, the correlation is good (0.85–0.96), so the spatial patterns agree well. In general, differences are highest in the mountains and lower in the plains. Here, we did not correct the precipitation data for snow (i.e., no consideration of precipitation on days below 0 °C), in contrast to the methodology of studies such as Johannsen et al. (2022) and Hanel et al. (2016b). This could explain parts of the differences, especially in the mountains. The differences could also be due to the different temporal coverage of the precipitation data used to generate the maps. The temporal coverage of our map (2001–2019) is very similar to that of the map by Auerswald et al. (2019a) (2001–2017) but agrees less with the temporal coverage of the maps of the other authors (1995–2015 for Johannsen et al., 2022; 1989–2003 for Hanel et al., 2016b; and 1970–2017 with a predominance of the last decade for Panagos et al., 2015b). Differences in temporal coverage are especially important given the observed increases in *R* factors in the last decades (e.g., Hanel et al., 2016a; Auerswald et al., 2019a, b). Furthermore, our methodology is very similar to that of Auerswald et al. (2019a) (e.g., calculation from contiguous data, hourly precipitation data, same temporal scaling factor and same equation used to calculate  $e_{\text{kin},i}$ ), whereas it differs from the methodology used by the other authors. The effect of using different equations to calculate  $e_{\text{kin},i}$  was investigated by Hanel et al. (2016b) and Nearing et al. (2017). The former authors found that average rainfall erosivity in the Czech Republic varied strongly between 500 and 760  $\text{MJ mm ha}^{-1} \text{h}^{-1}$  when 14 different equations were used. The USLE equation (which was used here) resulted in the highest values. Nearing et al. (2017) compared rainfall

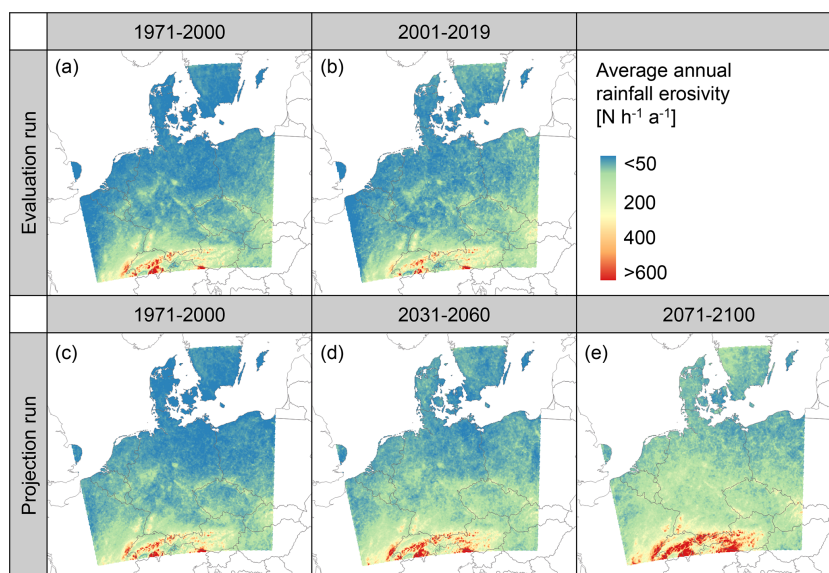


**Figure 2.** Average annual rainfall erosivity ( $R$  factor) in central Europe in the past, present and future derived from the evaluation run (a–b) and the historic and future projection simulations (c–e).

erosivity calculated with USLE, RUSLE (Brown and Foster, 1987, equation) and RUSLE2 and found that, on average, the values obtained with RUSLE and RUSLE2 were 14 % and 3.7 % lower than when USLE was used, respectively. A further important source of uncertainty is the choice of the scaling factors. Here, we used a temporal scaling factor of 1.90 that was established by Fischer et al. (2018) for Germany. This value is remarkably similar to the value of 1.87 established by Yue et al. (2020) for China. Keeping in mind that the temporal scaling factor of 1.56 established by Panagos et al. (2015b) for Europe was used for the conversion of 60 min data to 30 min data and that a second factor ( $0.80^{-1} = 1.25$ ) was established by the same authors for the conversion between 5 and 30 min data, the conversion factor is also similar. The assumption of a constant scaling factor for the entire model domain and the entire simulated time with different types of rain and shifting intensity patterns is certainly a simplification of reality that adds uncertainty. Here, we only used a temporal scaling factor and no spatial scaling factor because the results were in good agreement with those of Auerswald et al. (2019a). It is surprising that no spatial scaling factor was needed here, despite the resolution of 3 km that certainly smoothes sub-grid-scale variability in rainfall intensity and reduces local intensity peaks. Thus, other scaling factors, such as spatial scaling factors or bias correction between measured and simulated precipitation, might be necessary elsewhere, and the temporal scaling factor might have to be adapted to future data with higher intensities of extreme events.

In order to quantify the effect of using a different equation to calculate specific kinetic energy from rainfall intensity, we used a subset of our data (about 8 % of the model domain

located partly at the coast and partly in the Alps, covering 30 years from 1971 to 2000) to recalculate rainfall erosivity with the RUSLE equation. The USLE-based  $R$  factors are, on average, 1.23 times higher than those obtained with the RUSLE equation.

### 3.1.3 Seasonal distribution of rainfall erosivity

The seasonal distribution of rainfall erosivity shows a clear peak in the summer months (late-May–August; Fig. 4) and minima from November to March. This seasonal pattern is coherent with the results obtained by Johannsen et al. (2022) for Austria, by Auerswald et al. (2019a) for Germany and by Meusburger et al. (2012) for Switzerland. There is a strong variability from one day to another and between subregions of the modeling domain (light gray lines and dashed black line in Fig. 4). This is coherent with the observations made by Auerswald et al. (2019a) and can be explained by the effect of extreme rains that occur during the same day in several pixels (Auerswald et al., 2019a). Thus, single extreme rainfall events influence the mean values, despite the large number of pixels and the long averaging period of 30 years.

The smoothed distribution of the erosion index does not differ considerably between the past, the near future and the far future (Fig. 4). However, a comparison between past and present rainfall erosivity in Germany by Auerswald et al. (2019b) showed that winter erosivity increased considerably. In Switzerland, on the other hand, Meusburger et al. (2012) observed a decreasing trend in rainfall erosivity in February and an increase from May to October. The reasons for the discrepancies between this study, which did not detect significant changes in the seasonal distribution, and the other

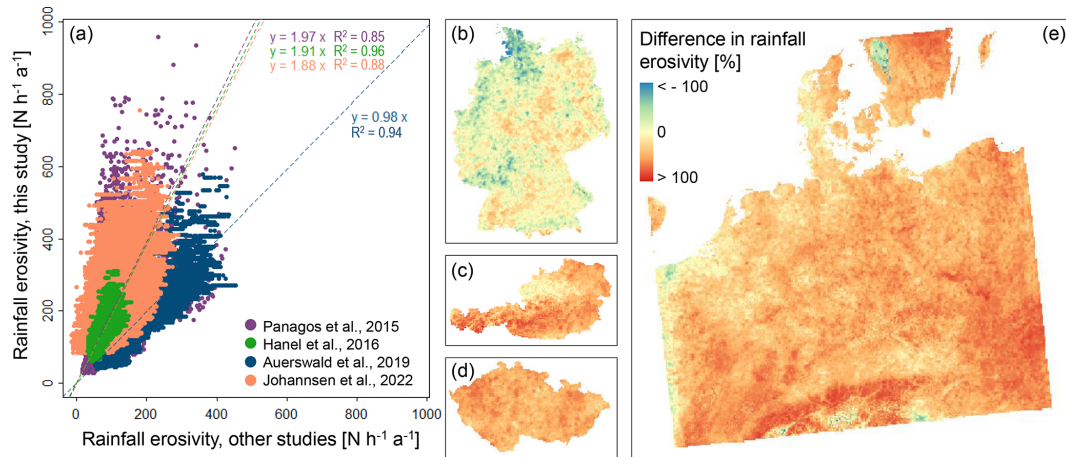


**Figure 3.** Comparison of the present rainfall erosivity map generated here (evaluation run, data from 2001 to 2019) with maps presented by other authors. In panel (a), each point corresponds to a raster cell; the dashed lines show the linear models fit to the data. Panels (b)–(e) show maps of differences between the map presented here and (b) the map for Germany by Auerswald et al. (2019a) covering the years 2001–2017, (c) the map for Austria by Johannsen et al. (2022) covering the years 1995–2015, (d) the map for the Czech Republic by Hanel et al. (2016b) covering the years 1989–2003 and (e) the map for central Europe by Panagos et al. (2015b) covering the years 1970–2017 with a predominance of the last decade.

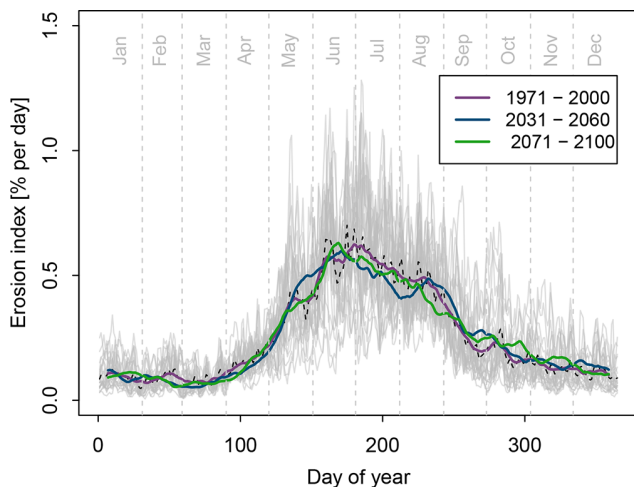


**Figure 4.** Seasonal distribution of the erosion index. The light gray lines show daily erosion indexes averaged over 30 years in the past (CPS-hist, 1971–2000) and in 25 subregions of the modeling domain. The dashed black line is the average of the entire modeling domain in the past, and the colored lines show the 13 d moving average for each one of the data sets for the past (CPS-hist, 1971–2000), the near future (CPS-scen-nf, 2031–2060) and the far future (CPS-scen-ff, 2071–2100).

studies that did observe trends are not clear yet and remain an open question.

### 3.2 Past and future changes in rainfall erosivity

In the evaluation run, average annual rainfall erosivity increased between the past (1971–2000, mean of  $90.5 \text{ N h}^{-1} \text{ a}^{-1}$ ) and the present (2001–2019, mean of  $97.8 \text{ N h}^{-1} \text{ a}^{-1}$ ) (Fig. 5). In the projection runs driven by the global climate model, rainfall erosivity increased considerably. This is the case for all statistics (Fig. 5). Mean values increased from  $96.3 \text{ N h}^{-1} \text{ a}^{-1}$  in the past to  $119.3 \text{ N h}^{-1} \text{ a}^{-1}$  in the near future and to  $149.7 \text{ N h}^{-1} \text{ a}^{-1}$  in the far future. Relative changes in average annual rainfall erosivity (in %) between the historical period and the near or far future are highest in the central and northern parts of the modeling domain, i.e., in the basins of the Weser, Ems and Elbe rivers and in the coastal basins in the north (Fig. 6a, e) where rainfall erosivity in the far future can be up to 84 % higher than in the past. Absolute changes, on the other hand, are highest in the basins of the Rhine ( $28 \text{ N h}^{-1} \text{ a}^{-1}$  in the near future and  $78 \text{ N h}^{-1} \text{ a}^{-1}$  in the far future) and the upper Danube ( $37$  and  $74 \text{ N h}^{-1} \text{ a}^{-1}$ , respectively). These are very strong changes. Furthermore, the changes in rainfall erosivity calculated from convection-permitting climate model output are considerably higher than those calculated with the low-resolution approach using mean annual precipitation from model output of conventional RCM ensembles (Fig. 6).

This is the case not only when future MAP is obtained from the median of the model ensemble but also for the entire plausible bandwidth of models. Figure 6 shows changes in rainfall erosivity estimated with the 15th and the 85th percentiles of the model ensemble. Even though this approach only considers changes in MAP and not changes in rainfall intensity, it allows an estimate of model uncertainty due



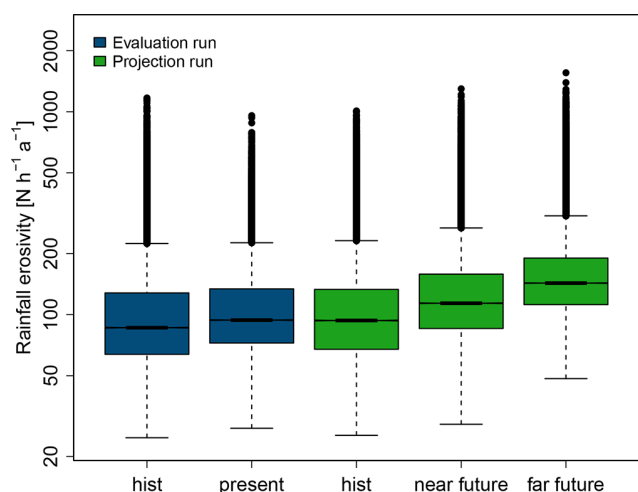


**Figure 5.** Distribution of the average annual rainfall erosivity ( $R$  factor) ( $\text{N h}^{-1} \text{a}^{-1}$ ) in the five data sets.

to the differences between the ensemble members. The results obtained with CPSs are outside of the bandwidth of the model ensemble because they also represent changes in extreme precipitation in addition to changes in MAP.

The finding that the low-resolution approach underestimates future changes in erosivity is in line with the results of Gericke et al. (2019). The regression equation of the German DIN 19708 that was used here (Eq. 3) was established in the early 1990s with climate data from the 1960s to the 1980s. Thus, changes in precipitation characteristics and the fact that it does not consider heavy precipitation raise concerns about using the equation on future data (Gericke et al., 2019). It has to be noted that DIN 19708 explicitly states that, whenever possible, high-frequency precipitation should be used and that Eq. (3) should only be used when only monthly or annual precipitation is available.

Annual rainfall erosivity in all topographic regions of central Europe (coasts, plains, low mountain ranges, Prealps and Alps) shows a strong interannual variability and clear trends (Fig. 7). The high interannual variability observed here is consistent with the findings of other authors, who observed strong interannual variability in rainfall erosivity calculated from measured precipitation data (e.g., Verstraeten et al., 2006; Meusburger et al., 2012; Fiener et al., 2013). The presence of trends supports the conclusions made by other authors: rainfall erosivity maps have to be frequently updated because old rainfall erosivity maps no longer represent current precipitation characteristics (Yin et al., 2017; Auerswald et al., 2019b; Johannsen et al., 2022).

While calculating future rainfall erosivity from CPSs offers the advantage of the direct calculation from high-resolution data, it only represents future projections from one model and one emission scenario, which is less robust than using model ensembles. Thus, we compared the past and future changes calculated here to observed and simu-

lated trends in rainfall erosivity in central Europe reported in the literature (Table S1). Both in the past and in the future, the range of reported trends is very large. The values given here agree well with reported values in some cases (e.g., approx. 20 % increase per decade in the Ruhr area of Germany calculated here for the projection run and reported by Fiener et al., 2013, in the 1973–2007 period). In other cases, they are strongly over- or underestimated (Table S1). It also has to be noted that, for the 1971–2000 period, for which we estimated rainfall erosivity from the projection run as well as from the evaluation run, the trends in the two data sets can differ considerably. In most regions, the changes were stronger in the projection run than in the evaluation run.

The high range of trends reported in the literature shows the need to consider model ensembles and to conduct sensitivity analyses to differences in methodology in future research. A comparison with the literature suggests that actual future changes could even be higher than reported here. Such strong changes in rainfall erosivity in the order of > 10 % per decade, as reported by Panagos et al. (2017, 2022), would have important implication for future soil erosion as well as for the occurrence of other natural risks such as landslides and flash floods that are triggered by heavy-rain events.

### 3.3 Potential and limitations of convection-permitting climate simulations for the calculation of rainfall erosivity

The maps presented here offer a high potential for erosion modeling and climate impact studies. Due to the high resolution of 3 km, they can represent the high spatial variability in rainfall erosivity in a large domain in central Europe. Unlike most other  $R$ -factor maps (e.g., Meusburger et al., 2012; Panagos et al., 2015b; Hanel et al., 2016b), our maps do not rely on spatial interpolation and correlation with other spatial covariates such as elevation, latitude, longitude or climate indices.

Because of the high temporal resolution of the underlying precipitation data, we did not have to rely on correlations between  $R$  factors calculated at a high resolution and low-resolution rainfall totals such as MAP. Many studies find a good correlation between MAP and  $R$  factors, suggesting that MAP is a good covariate to estimate  $R$  at locations where no high-resolution precipitation data are available. However, using empirical relations between past MAP and past  $R$  factors to derive future  $R$  factors is problematic, as it is unlikely that these relations remain stationary in the future (Quine and Van Oost, 2020). These relations are strongly conditioned by the frequency and magnitude of rainfall events that will very likely change in a warmer climate. In several regions in Europe, such as the Mediterranean (Tramblay et al., 2012; Blanchet et al., 2018) and the Carpathian Basin (Bartholy and Pongrácz, 2007), MAP is decreasing while extreme precipitation is increasing. This leads to an underestimation of future  $R$  factors that are derived from MAP alone. In central

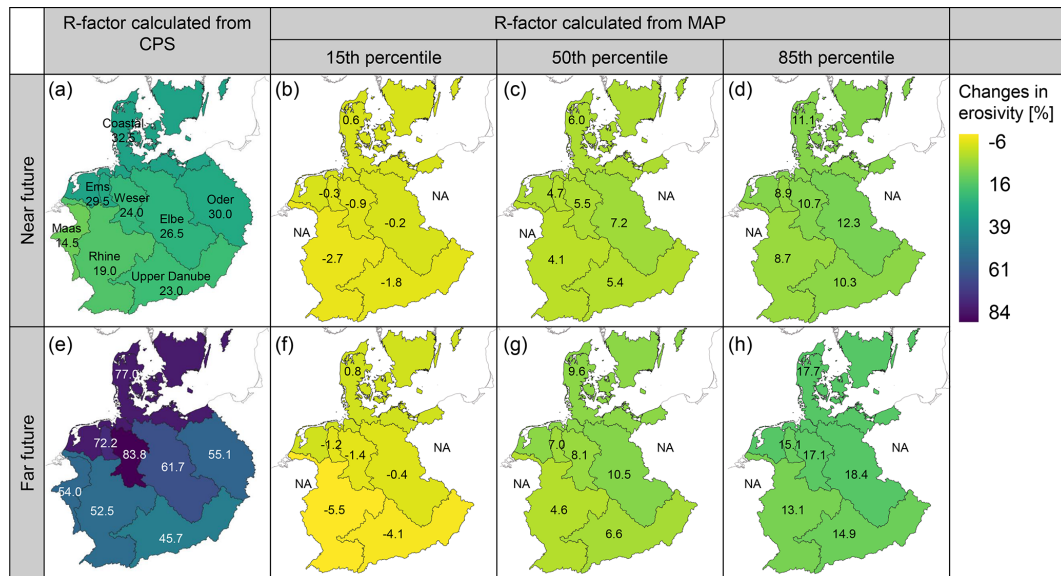


**Figure 6.** Relative changes in the average annual rainfall erosivity ( $R$  factor) in the major central European river basins between the historical period (1971–2000) and the near future (2031–2060, **a–d**) or the far future (2071–2100, **e–h**). All values are given as a percentage of the erosivity of the historical period. Panels (**a**) and (**e**) show changes in erosivity calculated with the convection-permitting simulations (CPSs); the other panels show changes in erosivity calculated with mean annual precipitation (MAP) obtained from the 15th, 50th and 85th percentiles of 21 regional climate models. All simulations used the RCP8.5 emission scenario.

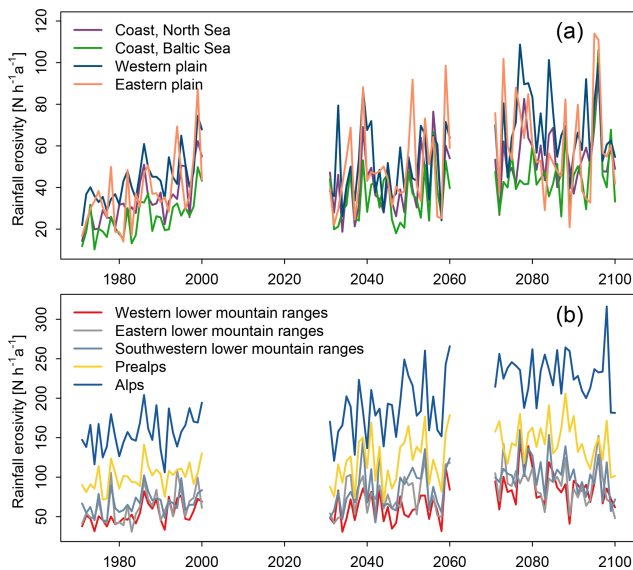


**Figure 7.** Trends and interannual variability in rainfall erosivity in the natural regions of central Europe for (**a**) the coast and plains and for (**b**) the lower mountain ranges, Prealps and Alps. Rainfall erosivity was calculated with precipitation data from the projection run. The natural regions were defined according to Bundesamt für Naturschutz (2017) for Germany and were manually extended to include central Europe based on elevation here. They are outlined in Fig. 1.

Europe, both MAP and extreme precipitation are expected to increase (Jacob et al., 2014; Brienens et al., 2020); thus, future  $R$  factors derived from MAP are also underestimated, although less severely than in the abovementioned regions. Because changes in MAP as well as in extreme precipitation are well represented in CPSs, they offer a valuable data source for the calculation of future rainfall erosivity.

Even when the same temporal resolution (3 h) of simulated precipitation data was compared, Chapman et al. (2021) found that rainfall erosivity was considerably higher and observed storm characteristics agreed better with simulated ones when a convection-permitting model was used instead of a conventional convection-parameterized one.

On the other hand, the maps presented here also have limitations. Here, we calculated rainfall erosivity from precipitation data and did not consider whether precipitation falls as rain, snow or hail; therefore, the high erosivity of hail is underestimated, while erosivity in zones where considerable amounts of precipitation fall as snow (i.e., mainly the Alps) is overestimated. As rainfall erosivity in central Europe is highest in the summer months, we assume that the impact of snow is small and can be neglected. For the Alps, this is not the case; thus, the very high values calculated in this region are too high.

As our maps are calculated from model output and not from precipitation measurements, the uncertainties in the model are propagated to the rainfall erosivity maps. The precipitation data were quality controlled and compared to radar- and station-based precipitation data from the past but

not bias corrected. The data showed a good agreement for extreme rainfall intensities for durations of more than 12 h but an overestimation for hourly extreme precipitation intensities (Rybka et al., 2022). This leads to an overestimation of the rainfall erosivity presented here that has to be kept in mind. Thus, it is important to compare the  $R$  factors calculated here to the ones calculated from measured rainfall data.

Concerning the future projections, it has to be noted that current climate models struggle with estimates of future precipitation, and biases are much larger than those for future temperatures (e.g., Slingo et al., 2022). Ensembles of global and regional climate models show a high range of future trends in precipitation that cannot be represented by a single model. Other studies estimated future  $R$  factors from ensembles of global or regional climate models such as the CMIP5 model ensemble, the model ensemble from the European part of the Coordinated Downscaling Experiment (EURO-CORDEX) or the DWD reference ensemble (Gerick et al., 2019; Panagos et al., 2022; Uber et al., 2022). In this way, the high range of projections can be represented and the uncertainty due to the choice of climate model and emission scenario can be assessed. Currently, such evaluations of variability between climate models are not possible for convection-permitting climate models, as no model ensembles of multi-decadal simulations over large domains are available. In COSMO-CLM, so far, only simulations driven with RCP8.5 have been performed; therefore, no data driven with the other emission scenarios are available. However, there are promising flagship studies such as the flagship pilot studies (FPS) from the CORDEX initiative, in which a first multi-model convection-permitting ensemble for the Alps and the Mediterranean is presented (Coppola et al., 2020). Furthermore, the latest generation of Coupled Model Inter-comparison Project Phase 6 (CMIP6) global climate models suggests that the decrease in summer precipitation in central Europe might be stronger than previously estimated by the CMIP5 model ensemble (Palmer et al., 2021; Ritzhaupt and Maraun, 2023), but these global models are only being downscaled by regional models now. Thus, the soil erosion modeling community should closely follow the coming advances in convection-permitting modeling to take advantage of new climate simulations for climate impact studies.

#### 4 Conclusions

We calculated rainfall erosivity (quantified as the USLE  $R$  factor) in central Europe in the past (1971–2000), present (2001–2019), near future (2031–2060) and far future (2071–2100) from convection-permitting simulation (CPS) output. From this work, we draw three main conclusions:

- Thanks to the high spatiotemporal resolution of CPSs (in this case 3 km and 1 h),  $R$  factors can be calculated directly without having to rely on spatial interpolation and regression with aggregated precipitation sums such

as mean annual precipitation (MAP). Thus, CPSs offer a high potential for the calculation of future  $R$  factors for climate impact studies on soil erosion. For the present, the  $R$ -factor map presented here is very similar to the map by Auerswald et al. (2019a) that was calculated from radar-derived precipitation data.

- In the river basins in central Europe, assuming the RCP8.5 emission scenario, changes in rainfall erosivity between the past and the near future can be as high as 33 %, whereas they can be up to 84 % higher in the far future. These rates of change are much higher than estimated previously using regression with MAP. This is due to the fact that the intensification of extreme precipitation is not represented by changes in MAP. This indicates that correlations between  $R$  factors and MAP that were developed in the past are not necessarily valid in the future.
- A major limitation of CPSs is their high computational demand. Thus, model domains are usually limited to much smaller spatial extents than those covered by global or regional climate models or the simulated time periods are limited to short time periods. The simulations in COSMO-CLM cover a long time period (109 years in total) and a comparably large modeling domain of approx.  $1.6 \times 10^6$  km<sup>2</sup> on land. However, to date, no ensembles of CPSs are available at the regional scale and for long time periods. Thus, in contrast to global or regional climate models, the uncertainty in future  $R$  factors due to the choice of climate models cannot yet be estimated by using a bandwidth of model ensembles. Promising advances in the CPS community – including flagship studies on CPS model ensembles – suggest that, in the future, more CPSs will be available for climate impact studies on soil erosion.

*Data availability.* The COSMO-CLM model output (e.g., hourly precipitation) is freely available from the CPS-eval evaluation simulations (<https://esgf.dwd.de/projects/dwd-cps/hoklisim-v2022-01>, Brienen et al., 2022), the CPS-hist historical projection simulations (<https://esgf.dwd.de/projects/dwd-cps/cps-hist-v2022-01>, Haller et al., 2022a) and the CPS-scen scenario projection simulations (<https://esgf.dwd.de/projects/dwd-cps/cps-scen-v2022-01>, Haller et al., 2022b). The rainfall erosivity maps presented in Fig. 2 are available at <https://doi.org/10.5281/zenodo.7628957> (Uber et al., 2023). Erosion index data can be provided upon request by the first author.

*Supplement.* The supplement related to this article is available online at: <https://doi.org/10.5194/hess-28-87-2024-supplement>.

*Author contributions.* MU and GH conceived and designed the study with contributions from all co-authors. MU performed the analyses and calculations with contributions from TH, CB and MH.

MH performed the simulations with COSMO-CLM and provided data. MU wrote the original draft with contributions from MH. MU created the figures. GH, TH and CB reviewed and edited the draft. GH acquired funding and was responsible for project administration.

*Competing interests.* The contact author has declared that none of the authors has any competing interests.

*Disclaimer.* Publisher's note: Copernicus Publications remains neutral with regard to jurisdictional claims made in the text, published maps, institutional affiliations, or any other geographical representation in this paper. While Copernicus Publications makes every effort to include appropriate place names, the final responsibility lies with the authors.

*Acknowledgements.* The authors wish to thank their colleagues at the Federal Institute of Hydrology (BfG) and DWD as well as the members of the Network of Experts Themenfeld 1 for fruitful discussions. R-factor calculations were run on the BfG's high-performance computers. We thank the maintainers and users for the provision of the infrastructure and their useful advice. COSMO-CLM is a regional climate model maintained by the CLM-Community. We thank the community members for their support. Furthermore, we thank the editor, the three anonymous referees and the researchers who participated in the active, open discussion for their feedback and comments that helped greatly to improve the quality of this paper.

*Financial support.* This research was funded by the German Federal Ministry for Digital and Transport Network of Experts.

*Review statement.* This paper was edited by Nadav Peleg and reviewed by three anonymous referees.

## References

- Alexander, L. V., Zhang, X., Peterson, T. C., Caesar, J., Gleason, B., Klein Tank, A., Haylock, M., Collins, D., Trewin, B., Rahimzadeh, F., Tagipour, A., Rupa Kumar, K., Revadekar, J., Griffiths, G., Vincent, L., Stephenson, D. B., Burn, J., Aguilar, E., Brunet, M., Taylor, M., New, M., Zhai, P., Rusticucci, M., and Vazquez-Aguirre, J. L.: Global observed changes in daily climate extremes of temperature and precipitation, *J. Geophys. Res.-Atmos.*, 111, D05109, <https://doi.org/10.1029/2005JD006290>, 2006.
- Allan, R. P., Barlow, M., Byrne, M. P., Cherchi, A., Douville, H., Fowler, H. J., Gan, T. Y., Pendergrass, A. G., Rosenfeld, D., Swann, A. L. S., Wilcox, L. J., and Zolina, O.: Advances in understanding large-scale responses of the water cycle to climate change, *Ann. NY Acad. Sci.*, 1472, 49–75, <https://doi.org/10.1111/nyas.14337>, 2020.
- Allen, M. R. and Ingram, W. J.: Constraints on future changes in climate and the hydrologic cycle, *Nature*, 419, 224–232, <https://doi.org/10.1038/nature01092>, 2002.
- Amundson, R., Berhe, A. A., Hopmans, J. W., Olson, C., Sztein, A. E., and Sparks, D. L.: Soil and human security in the 21st century, *Science*, 348, 1261071, <https://doi.org/10.1126/science.1261071>, 2015.
- Arnone, E., Pumo, D., Viola, F., Noto, L. V., and La Loggia, G.: Rainfall statistics changes in Sicily, *Hydrol. Earth Syst. Sci.*, 17, 2449–2458, <https://doi.org/10.5194/hess-17-2449-2013>, 2013.
- Auerswald, K., Fischer, F. K., Winterrath, T., and Brandhuber, R.: Rain erosivity map for Germany derived from contiguous radar rain data, *Hydrol. Earth Syst. Sci.*, 23, 1819–1832, <https://doi.org/10.5194/hess-23-1819-2019a>.
- Auerswald, K., Fischer, F., Winterrath, T., Elhaus, D., Maier, H., and Brandhuber, R.: Klimabedingte Veränderung der Regenositivität seit 1960 und Konsequenzen für Bodenabtragsschätzungen, in: *Bodenschutz, Ergänzbare Handbuch der Maßnahmen und Empfehlungen für Schutz, Pflege und Sanierung von Böden, Landschaft und Grundwasser*, edited by: Bachmann G., König W., and Utermann J., Erich Schmidt Verlag, Berlin, Germany, 21 pp., ISBN 978-3-503-02718-7, 2019b.
- Ban, N., Schmidli, J., and Schär, C.: Evaluation of the convection-resolving regional climate modeling approach in decade-long simulations, *J. Geophys. Res.-Atmos.*, 119, 7889–7907, <https://doi.org/10.1002/2014JD021478>, 2014.
- Ban, N., Cécile, C., Coppola, E., Pichelli, E., Sobolowski, S., Adinolfi, M., Ahrens, B., Alias, A., Anders, I., Bastin, S., Belušić, D., Berthou, S., Brisson, E., Cardoso, R. M., Chan, S. C., Christensen, O. B., Fernández, J., Fita, L., Frisius, T., Gašparac, G., Giorgi, F., Goergen, K., Haugen, J. E., Hodnebrog, Ø., Kartios, S., Katragkou, E., Kendon, E. J., Keuler, K., Lavin-Gullon, A., Lenderink, G., Leutwyler, D., Lorenz, T., Maraun, D., Mergogliano, P., Milovac, J., Panitz, H.-J., Raffa, M., Remedio, A. R., Schär, C., Soares, P. M. M., Srncic, L., Steensen, B. M., Stocchi, P., Tölle, M. H., Truhetz, H., Vergara-Temprado, J., de Vries, H., Warrach-Sagi, K., Wulfmeyer, V., and Zander, M. J.: The first multi-model ensemble of regional climate simulations at kilometer-scale resolution, part I: evaluation of precipitation, *Clim. Dynam.*, 57, 275–302, <https://doi.org/10.1007/s00382-021-05708-w>, 2021.
- Bartholy, J. and Pongrácz, R.: Regional analysis of extreme temperature and precipitation indices for the Carpathian Basin from 1946 to 2001, *Global Planet. Change*, 57, 83–95, <https://doi.org/10.1016/j.gloplacha.2006.11.002>, 2007.
- Berg, P., Moseley, C., and Haerter, J. O.: Strong increase in convective precipitation in response to higher temperatures, *Nat. Geosci.*, 6, 181–185, <https://doi.org/10.1038/ngeo1731>, 2013.
- Bilotta, G. S. and Brazier, R. E.: Understanding the influence of suspended solids on water quality and aquatic biota, *Water Res.*, 42, 2849–2861, <https://doi.org/10.1016/j.watres.2008.03.018>, 2008.
- Blanchet, J., Moliné, G., and Touati, J.: Spatial analysis of trend in extreme daily rainfall in southern France, *Clim. Dynam.*, 51, 799–812, 2018.
- Böhm, U., Kücken, M., Ahrens, W., Block, A., Hauße, D., Keuler, K., Rockel, B., and Will, A.: CLM-the climate version of LM: brief description and long-term applications, *COSMO newsletter*, 6, 225–235, 2006.

- Borrelli, P., Robinson, D. A., Panagos, P., Lugato, E., Yang, J. E., Alewell, C., Wuepper, D., Montanarella, L., and Ballabio, C.: Land use and climate change impacts on global soil erosion by water (2015–2070), *P. Natl. Acad. Sci. USA*, 117, 21994–22001, <https://doi.org/10.1073/pnas.2001403117>, 2020.
- Borrelli, P., Alewell, C., Alvarez, P., Anache, J. A. A., Baartman, J., Ballabio, C., Bezak, N., Biddoccu, M., Cerdà, A., Chalise, D., Chen, S., Chen, W., De Girolamo, A. M., Gessesse, G. D., Deumlich, D., Diodato, N., Efthimiou, N., Erpul, G., Fiener, P., Freppaz, M., Gentile, F., Gericke, A., Haregeweyn, N., Hu, B., Jeanneau, A., Kaffas, K., Kiani-Harchegani, M., Lizaga Villuendas, I., Li, C., Lombardo, L., López-Vicente, M., Lucas-Borja, M. E., Märker, M., Matthews, V., Miao, C., Mikoš, M., Modugno, S., Möller, M., Naipal, V., Nearing, M., Owusu, S., Panday, D., Patault, E., Patriche, C. V., Poggio, L., Portes, R., Quijano, L., Rahdari, M. R., Renima, M., Ricci, G. F., Rodrigo-Comino, J., Saia, S., Samani, A. N., Schillaci, C., Syrris, V., Kim, H. S., Spinola, D. N., Oliveira, P. T., Teng, H., Thapa, R., Vantas, K., Vieira, D., Yang, J. E., Yin, S., Zema, D. A., Zhao, G., and Panagos, P.: Soil erosion modelling: A global review and statistical analysis, *Sci. Total Environ.*, 780, 146494, <https://doi.org/10.1016/j.scitotenv.2021.146494>, 2021.
- Brienen, S., Water, A., Brendel, C., Fleischer, C., Ganske, A., Haller, M., Helms, M., Höpp, S., Jensen, C., Jochumsen, K., Möller, J., Krähenmann, S., Nilson, E., Rauthe, M., Razafimaharo, C., Rudolph, E., Rybka, H., Schade, N., and Stanley, K.: Klimawandelbedingten Änderungen in Atmosphäre und Hydrosphäre. Schlussbericht des Schwerpunktthemas Szenarienbildung (SP-101) im Themenfeld 1 des BMVI-Expertennetzwerk, 157 pp., <https://doi.org/10.5675/ExpNBS2020.2020.02>, 2020.
- Brienen, S., Haller, M., Brauch, J., and Früh, B.: HoKliSim-De evaluation simulation with COSMO-CLM5-0-16 version V2022.01, DWD [data set], <https://esgf.dwd.de/projects/dwd-cps/hoklisim-v2022-01> (last access: 3 January 2024), 2022.
- Brown, L. and Foster, C.: Storm erosivity using idealized intensity distributions, *T. ASAE*, 30, 378–386, 1987.
- Brychta, J., Podhrázská, J., and Štastná, M.: Review of methods of spatio-temporal evaluation of rainfall erosivity and their correct application, *Catena*, 217, 106454, <https://doi.org/10.1016/j.catena.2022.106454>, 2022.
- Bundesamt für Naturschutz: Naturräume und Großlandschaften Deutschlands (n.Ssymank), Bundesamt für Naturschutz [data set], <https://www.bfn.de/daten-und-fakten/biogeografische-regionen-und-naturraeumliche-haupteinheiten-deutschlands> (last access: 19 December 2023), 2017.
- Chapman, S., Birch, C. E., Galdos, M. V., Pope, E., Davie, J., Bradshaw, C., Eze, S., and Marsham, J. H.: Assessing the impact of climate change on soil erosion in East Africa using a convection-permitting climate model, *Environ. Res. Lett.*, 16, 084006, <https://doi.org/10.1088/1748-9326/ac10e1>, 2021.
- Ciszewski, D. and Grygar, T. M.: A review of flood-related storage and remobilization of heavy metal pollutants in river systems, *Water Air Soil Poll.*, 227, 239, <https://doi.org/10.1007/s11270-016-2934-8>, 2016.
- Copernicus Land Monitoring Service: European Digital Elevation Model (EU-DEM), version 1.1 (1.1), European Environment Agency [data set], <https://www.eea.europa.eu/en/datahub/datahubitem-view/d08852bc-7b5f-4835-a776-08362e2fbf4b> (last access: 19 December 2023), 2016.
- Coppola, E., Sobolowski, S., Pichelli, E., Raffaele, F., Ahrens, B., Anders, I., Ban, N., Bastin, S., Belda, M., Belusic, D., Caldas-Alvarez, A., Cardoso, R. M., Davolio, S., Dobler, A., Fernandez, J., Fita, L., Fumiere, Q., Giorgi, F., Goergen, K., Güttler, I., Halenka, T., Heinzeller, D., Hodnebrog, Ø., Jacob, D., Kartsios, S., Katragkou, E., Kendon, E., Khodayar, S., Kunstmann, H., Knist, S., Lavín-Gullón, A., Lind, P., Lorenz, T., Maraun, D., Marelle, L., van Meijgaard, E., Milovac, J., Myhre, G., Panitz, H. J., Piazza, M., Raffa, M., Raub, T., Rockel, B., Schär, C., Sieck, K., Soares, P. M. M., Somot, S., Srncic, L., Stocchi, P., Tölle, M. H., Truhetz, H., Vautard, R., de Vries, H., and Warrach-Sagi, K.: A first-of-its-kind multi-model convection permitting ensemble for investigating convective phenomena over Europe and the Mediterranean, *Clim. Dynam.*, 55, 3–34, <https://doi.org/10.1007/s00382-018-4521-8>, 2020.
- Coulthard, T. J., Ramirez, J., Fowler, H. J., and Glenis, V.: Using the UKCP09 probabilistic scenarios to model the amplified impact of climate change on drainage basin sediment yield, *Hydrol. Earth Syst. Sci.*, 16, 4401–4416, <https://doi.org/10.5194/hess-16-4401-2012>, 2012.
- DIN-Normenausschuss Wasserwesen: DIN 19708:2017-08 Bodenbeschaffenheit – Ermittlung der Erosionsgefährdung von Böden durch Wasser mit Hilfe der ABAG, <https://doi.org/10.31030/2676773>, 2017.
- Doms, G., Förstner, J., Heise, E., Herzog, H., Mironov, D., Raschendorfer, M., Reinhardt, T., Ritter, B., Schrodin, R., and Schulz, J.-P.: A description of the nonhydrostatic regional COSMO model, Part II: Physical Parameterization, Deutscher Wetterdienst, Offenbach, Germany, 177 pp., [http://www.cosmo-model.org/content/model/cosmo/coreDocumentation/cosmo\\_physics\\_4.20.pdf](http://www.cosmo-model.org/content/model/cosmo/coreDocumentation/cosmo_physics_4.20.pdf) (last access: 19 December 2023), 2011.
- Eekhout, J. P. C. and De Vente, J.: How soil erosion model conceptualization affects soil loss projections under climate change, *Prog. Phys. Geog.*, 44, 212–232, <https://doi.org/10.1177/0309133319871937>, 2020.
- Fiener, P., Neuhaus, P., and Botschek, J.: Long-term trends in rainfall erosivity – analysis of high resolution precipitation time series (1937–2007) from Western Germany, *Agr. Forest Meteorol.*, 171, 115–123, <https://doi.org/10.1016/j.agrformet.2012.11.011>, 2013.
- Fischer, E. M. and Knutti, R.: Observed heavy precipitation increase confirms theory and early models, *Nat. Clim. Change*, 6, 986–991, <https://doi.org/10.1038/nclimate3110>, 2016.
- Fischer, F. K., Winterrath, T., and Auerswald, K.: Temporal- and spatial-scale and positional effects on rain erosivity derived from point-scale and contiguous rain data, *Hydrol. Earth Syst. Sci.*, 22, 6505–6518, <https://doi.org/10.5194/hess-22-6505-2018>, 2018.
- Fowler, H. J., Lenderink, G., Prein, A. F., Westra, S., Allan, R. P., Ban, N., Barbero, R., Berg, P., Blenkinsop, S., Do, H. X., Guerreiro, S., Haerter, J. O., Kendon, E. J., Lewis, E., Schär, C., Sharma, A., Villarini, G., Wasko, C., and Zhang, X.: Anthropogenic intensification of short-duration rainfall extremes, *Nat. Rev. Earth Environ.*, 2, 107–122, <https://doi.org/10.1038/s43017-020-00128-6>, 2021.
- Gericke, A., Kiesel, J., Deumlich, D., and Venohr, M.: Recent and future changes in rainfall erosivity and implications for the soil erosion risk in Brandenburg, NE Germany, *Water-SUI*, 11, 904, <https://doi.org/10.3390/w11050904>, 2019.

- Giorgetta, M., Brokopf, R., Crueger, T., Esch, M., Fiedler, S., Helmet, J., Hohenegger, C., Kornblueh, L., Köhler, M., Manzini, E., Mauritsen, T., Nam, C., Raddatz, T., Rast, S., Reinert, D., Sakradzija, M., Schmidt, H., Schneck, R., Schnur, R., Silvers, L., Wan, H., Zängl, G., and Stevens, B.: ICON-A, the Atmosphere Component of the ICON Earth System Model: I. Model Description, *J. Adv. Model. Earth Sy.*, 10, 1613–1637, <https://doi.org/10.1029/2017MS001242>, 2018.
- Groisman, P. Y., Knight, R. W., Easterling, D. R., Karl, T. R., Hegerl, G. C., and Razuvaev, V. N.: Trends in intense precipitation in the climate record, *J. Climate*, 18, 1326–1350, <https://doi.org/10.1175/JCLI3339.1>, 2005.
- Haller, M., Brienens, S., Brauch, J., and Früh, B.: Historical simulation with COSMO-CLM5-0-16, version V2022.01, DWD [data set], <https://esgf.dwd.de/projects/dwd-cps/cps-hist-v2022-01> (last access: 3 January 2024), 2022a.
- Haller, M., Brienens, S., Brauch, J., and Früh, B.: Projection simulation with COSMO-CLM5-0-16, version V2022.01, DWD [data set], <https://esgf.dwd.de/projects/dwd-cps/cps-scen-v2022-01> (last access: 3 January 2024), 2022b.
- Hanel, M., Pavlásková, A., and Kyselý, J.: Trends in characteristics of sub-daily heavy precipitation and rainfall erosivity in the Czech Republic, *Int. J. Climatol.*, 36, 1833–1845, <https://doi.org/10.1002/joc.4463>, 2016a.
- Hanel, M., Máca, P., Bašta, P., Vlnas, R., and Pech, P.: The rainfall erosivity factor in the Czech Republic and its uncertainty, *Hydrol. Earth Syst. Sci.*, 20, 4307–4322, <https://doi.org/10.5194/hess-20-4307-2016>, 2016b.
- Hersbach, H., Bell, B., Berrisford, P., Hirahara, S., Horányi, A., Muñoz-Sabater, J., Nicolas, J., Peubey, C., Radu, R., Schepers, D., Simmons, A., Soci, C., Abdalla, S., Abellan, X., Balsamo, G., Bechtold, P., Biavati, G., Bidlot, J., Bonavita, M., De Chiara, G., Dahlgren, P., Dee, D., Diamantakis, M., Dragani, R., Flemming, J., Forbes, R., Fuentes, M., Geer, A., Haimberger, L., Healy, S., Hogan, R. J., Hólm, E., Janisková, M., Keeley, S., Laloyaux, P., Lopez, P., Lupu, C., Radnoti, G., de Rosnay, P., Rozum, I., Vamborg, F., Villaume, S., and Thépaut, J.-N.: The ERA5 global reanalysis, *Q. J. Roy. Meteor. Soc.* 146, 1999–2049, <https://doi.org/10.1002/qj.3803>, 2020.
- Jacob, D., Petersen, J., Eggert, B., Alias, A., Christensen, O. B., Bouwer, L. M., Braun, A., Colette, A., Déque, M., Georgievski, G., Georgopoulou, E., Gobiet, A., Menut, L., Nikulin, G., Haensler, A., Hempelmann, N., Jones, C., Keuler, K., Kovats, S., Kröner, N., Kotlarski, S., Kriegsmann, A., Martin, E., van Meijgaard, E., Moseley, C., Pfeifer, S., Preuschmann, S., Radermacher, C., Radtke, K., Rechid, D., Rounsevell, M., Samuelsson, P., Somot, S., Soussana, J.-F., Teichmann, C., Valentini, R., Vautard, R., Weber, B., and Yiou, P.: EURO-CORDEX: new high-resolution climate change projections for European impact research, *Reg. Environ. Change*, 14, 563–578, <https://doi.org/10.1007/s10113-013-0499-2>, 2014.
- Johannsen, L. L., Schmaltz, E. M., Mitrovits, O., Klik, A., Smoliner, W., Wang, S., and Strauss, P.: An update of the spatial and temporal variability of rainfall erosivity (*R*-factor) for the main agricultural production zones of Austria, *Catena*, 215, 106305, <https://doi.org/10.1016/j.catena.2022.106305>, 2022.
- Kendon, E. J., Roberts, N. M., Fowler, H. J., Roberts, M. J., Chan, S. C., and Senior, C. A.: Heavier summer downpours with climate change revealed by weather forecast resolution model, *Nat. Clim. Change*, 4, 570–576, <https://doi.org/10.1038/nclimate2258>, 2014.
- Kendon, E. J., Ban, N., Roberts, N. M., Fowler, H. J., Roberts, M. J., Chan, S. C., Evans, J. P., Fosser, G., and Wilkinson, J. M.: Do convection-permitting regional climate models improve projections of future precipitation change?, *B. Am. Meteorol. Soc.*, 98, 79–93, <https://doi.org/10.1175/BAMS-D-15-0004.1>, 2017.
- Kharin, V. V., Zwiers, F. W., Zhang, X., and Wehner, M.: Changes in temperature and precipitation extremes in the CMIP5 ensemble, *Clim. Change*, 119, 345–357, <https://doi.org/10.1007/s10584-013-0705-8>, 2013.
- Kondolf, G. M., Gao, Y., Annandale, G. W., Morris, G. L., Jiang, E., Zhang, J., Cao, Y., Carling, P., Fu, K., Guo, Q., Hotchkiss, R., Peteuil, C., Sumi, T., Wang, H. W., Wang, Z., Wei, Z., Wu, B., Wu, C., and Yang, C. T.: Sustainable sediment management in reservoirs and regulated rivers: experiences from five continents, *Earths Future*, 2, 256–280, <https://doi.org/10.1002/2013EF000184>, 2014.
- Kreklow, J., Steinhoff-Knopp, B., Friedrich, K., and Tetzlaff, B.: Comparing rainfall erosivity estimation methods using weather radar data for the State of Hesse (Germany), *Water-SUI*, 12, 1424, <https://doi.org/10.3390/w12051424>, 2020.
- Laws, J. O. and Parsons, A.: The relation of raindrop-size to intensity, *EOS T. Am. Geophys. Un.*, 24, 452–460, <https://doi.org/10.1029/TR024i002p00452>, 1943.
- Lucas-Picher, P., Argüeso, D., Brisson, E., Trambly, Y., Berg, P., Lemonsu, A., Kotlarski, S., and Caillaud, C.: Convection-permitting modeling with regional climate models: Latest developments and next steps, *WIRES Clim. Change*, 12, e731, <https://doi.org/10.1002/wcc.731>, 2021.
- Meusburger, K., Steel, A., Panagos, P., Montanarella, L., and Alewell, C.: Spatial and temporal variability of rainfall erosivity factor for Switzerland, *Hydrol. Earth Syst. Sci.*, 16, 167–177, <https://doi.org/10.5194/hess-16-167-2012>, 2012.
- Mueller, E. N. and Pfister, A.: Increasing occurrence of high-intensity rainstorm events relevant for the generation of soil erosion in a temperate lowland region in Central Europe, *J. Hydrol.*, 411, 266–278, <https://doi.org/10.1016/j.jhydrol.2011.10.005>, 2011.
- Mueller, M., Bierschenk, A. M., Bierschenk, B. M., Pander, J., and Geist, J.: Effects of multiple stressors on the distribution of fish communities in 203 headwater streams of Rhine, Elbe and Danube, *Sci. Total Environ.*, 703, 134523, <https://doi.org/10.1016/j.scitotenv.2019.134523>, 2020.
- Nearing, M. A., Pruski, F. F., and O’Neal, M. R.: Expected climate change impacts on soil erosion rates: A review, *J. Soil Water Conserv.*, 59, 43–50, 2004.
- Nearing, M. A., Yin, S.-Q., Borrelli, P., and Polyakov, V. O.: Rainfall erosivity: An historical review, *Catena*, 157, 357–362, <https://doi.org/10.1016/j.catena.2017.06.004>, 2017.
- Orgiazzi, A. and Panagos, P.: Soil biodiversity and soil erosion: It is time to get married: Adding an earthworm factor to soil erosion modelling, *Global Ecol. Biogeogr.*, 27, 1155–1167, <https://doi.org/10.1111/geb.12782>, 2018.
- Owens, P. N., Batalla, R. J., Collins, A. J., Gomez, B., Hicks, D. M., Horowitz, A. J., Kondolf, G. M., Marden, M., Page, M. J., Peacock, D. H., Petticrew, E. L., Salomons, W., and Trustrum, N. A.: Fine-grained sediment in river systems: Environmental signifi-

- cance and management issues, *River Res. Appl.*, 21, 693–717, <https://doi.org/10.1002/rra.878>, 2005.
- Palmer, T. E., Booth, B. B. B., and McSweeney, C. F.: How does the CMIP6 ensemble change the picture for European climate projections?, *Environ. Res. Lett.*, 16, 094042, <https://doi.org/10.1088/1748-9326/ac1ed9>, 2021.
- Panagos, P., Borrelli, P., Poesen, J., Ballabio, C., Lugato, E., Meusburger, K., Montanarella, L., and Alewell, C.: The new assessment of soil loss by water erosion in Europe, *Environ. Sci. Policy*, 54, 438–447, <https://doi.org/10.1016/j.envsci.2015.08.012>, 2015a.
- Panagos, P., Ballabio, C., Borrelli, P., Meusburger, K., Klik, A., Rousseva, S., Tadić, M. P., Michaelides, S., Hrabalíková, M., and Olsen, P.: Rainfall erosivity in Europe, *Sci. Total Environ.*, 511, 801–814, <https://doi.org/10.1016/j.scitotenv.2015.01.008>, 2015b.
- Panagos, P., Ballabio, C., Meusburger, K., Spinoni, J., Alewell, C., and Borrelli, P.: Towards estimates of future rainfall erosivity in Europe based on REDES and WorldClim datasets, *J. Hydrol.*, 548, 251–262, <https://doi.org/10.1016/j.jhydrol.2017.03.006>, 2017.
- Panagos, P., Borrelli, P., Matthews, F., Liakos, L., Bezak, N., Diodato, N., and Ballabio, C.: Global rainfall erosivity projections for 2050 and 2070, *J. Hydrol.*, 610, 127865, <https://doi.org/10.1016/j.jhydrol.2022.127865>, 2022.
- Pham, T. V., Steger, C., Rockel, B., Keuler, K., Kirchner, I., Mertens, M., Rieger, D., Zängl, G., and Früh, B.: ICON in Climate Limited-area Mode (ICON release version 2.6.1): a new regional climate model, *Geosci. Model Dev.*, 14, 985–1005, <https://doi.org/10.5194/gmd-14-985-2021>, 2021.
- Phinzi, K. and Ngetar, N. S.: The assessment of water-borne erosion at catchment level using GIS-based RUSLE and remote sensing: A review, *International Soil and Water Conservation Research*, 7, 27–46, <https://doi.org/10.1016/j.iswcr.2018.12.002>, 2019.
- Pierce, D.: Package “ncdf4”, CRAN [code], <https://cran.r-project.org/web/packages/ncdf4/index.html>, 2019.
- Pimentel, D., Harvey, C., Resosudarmo, P., Sinclair, K., Kurz, D., McNair, M., Crist, S., Shpritz, L., Fitton, L., and Safouri, R.: Environmental and economic costs of soil erosion and conservation benefits, *Science*, 267, 1117–1123, <https://doi.org/10.1126/science.267.5201.1117>, 1995.
- Prein, A. F., Langhans, W., Fosser, G., Ferrone, A., Ban, N., Gørgen, K., Keller, M., Tölle, M., Gutjahr, O., Feser, F., Brisson, E., Kollet, S., Schmidli, J., van Lipzig, N. P. M., and Leung, R.: A review on regional convection-permitting climate modeling: Demonstrations, prospects, and challenges, *Rev. Geophys.*, 53, 323–361, <https://doi.org/10.1002/2014RG000475>, 2015.
- Quine, T. A. and Van Oost, K.: Insights into the future of soil erosion, *P. Natl. Acad. Sci. USA*, 117, 23205–23207, <https://doi.org/10.1073/pnas.2017314117>, 2020.
- Raffa, M., Reder, A., Adinolfi, M., and Mercogliano, P.: A comparison between one-step and two-step nesting strategy in the dynamical downscaling of regional climate model COSMO-CLM at 2.2 km driven by ERA5 reanalysis, *Atmosphere-Basel*, 12, 260, <https://doi.org/10.3390/atmos12020260>, 2021.
- Renard, K. G., Foster, G. R., Weesies, G. A., McCool, D. K., and Yoder, D. C.: Predicting soil erosion by water: A guide to conservation planning with the Revised Universal Soil Loss Equation (RUSLE), *Agriculture Handbook*, 703, United States Department of Agriculture, 407 pp., [https://www.ars.usda.gov/arsuserfiles/64080530/rusle/ah\\_703.pdf](https://www.ars.usda.gov/arsuserfiles/64080530/rusle/ah_703.pdf) (last access: 19 December 2023), 1993.
- Risal, A., Lim, K. J., Bhattarai, R., Yang, J. E., Noh, H., Pathak, R., and Kim, J.: Development of web-based WERM-S module for estimating spatially distributed rainfall erosivity index (EI30) using RADAR rainfall data, *Catena*, 161, 37–49, <https://doi.org/10.1016/j.catena.2017.10.015>, 2018.
- Ritzhaupt, N. and Maraun, D.: Consistency of Seasonal Mean and Extreme Precipitation Projections Over Europe Across a Range of Climate Model Ensembles, *J. Geophys. Res.-Atmos.*, 128, e2022JD037845, <https://doi.org/10.1029/2022JD037845>, 2023.
- Rockel, B., Will, A., and Hense, A.: The regional climate model COSMO-CLM (CCLM), *Meteorol. Z.*, 17, 347, <https://doi.org/10.1127/0941-2948/2008/0309>, 2008.
- Rogler, H. and Schwertmann, U.: Erosivität der Niederschläge und Isoerodentkarte Bayerns, *Zeitung für Kulturtechnik und Flurbereinigung*, 22, 99–112, 1981.
- Routschek, A., Schmidt, J., and Kreienkamp, F.: Climate Change impacts on soil erosion: A high-resolution projection on catchment scale until 2100, in *Engineering Geology for Society and Territory*, Vol. 1, edited by: Lollino, G., Manconi, A., Clague, J., Shan, W., and Chiarle, M., Springer, Cham., 135–141, [https://doi.org/10.1007/978-3-319-09300-0\\_26](https://doi.org/10.1007/978-3-319-09300-0_26), 2015.
- Rybka, H., Haller, M., Brienens, S., Brauch, J., Früh, B., Junghänel, T., Lengfeld, K., Walter, A., and Winterrath, T.: Convection-permitting climate simulations with COSMO-CLM for Germany: Analysis of present and future daily and sub-daily extreme precipitation, development, *Meteorol. Z.*, 64, 91–111, <https://doi.org/10.1127/metz/2022/1147>, 2022.
- Sartori, M., Philippidis, G., Ferrari, E., Borrelli, P., Lugato, E., Montanarella, L., and Panagos, P.: A linkage between the biophysical and the economic: Assessing the global market impacts of soil erosion, *Land Use Policy*, 86, 299–312, <https://doi.org/10.1016/j.landusepol.2019.05.014>, 2019.
- Schulzweida, U.: CDO User Guide (2.1.0), Zenodo [code], <https://doi.org/10.5281/zenodo.7112925>, 2022.
- Scoccimarro, E., Gualdi, S., Bellucci, A., Zampieri, M., and Navarra, A.: Heavy precipitation events in a warmer climate: Results from CMIP5 models, *J. Climate*, 26, 7902–7911, <https://doi.org/10.1175/JCLI-D-12-00850.1>, 2013.
- Simonneau, V., Cheggour, A., Deschamps, C., Mouillot, F., Cerdan, O., and Le Bissonnais, Y.: Land use and climate change effects on soil erosion in a semi-arid mountainous watershed (High Atlas, Morocco), *J. Arid Environ.*, 122, 64–75, <https://doi.org/10.1016/j.jaridenv.2015.06.002>, 2015.
- Slingo, J., Bates, P., Bauer, P., Belcher, S., Palmer, T., Stephens, G., Stevens, B., Stocker, T., and Teutsch, G.: Ambitious partnership needed for reliable climate prediction, *Nat. Clim. Change*, 12, 499–503, <https://doi.org/10.1038/s41558-022-01384-8>, 2022.
- Sørland, S. L., Brogli, R., Pothapakula, P. K., Russo, E., Van de Walle, J., Ahrens, B., Anders, I., Bucchignani, E., Davin, E. L., Demory, M.-E., Dosio, A., Feldmann, H., Früh, B., Geyer, B., Keuler, K., Lee, D., Li, D., van Lipzig, N. P. M., Min, S.-K., Panitz, H.-J., Rockel, B., Schär, C., Steger, C., and Thiery, W.: COSMO-CLM regional climate simulations in the Coordinated Regional Climate Downscaling Experiment (CORDEX) framework: a review, *Geosci. Model Dev.*, 14, 5125–5154, <https://doi.org/10.5194/gmd-14-5125-2021>, 2021.

- Stefanidis, S., Alexandridis, V., and Ghosal, K.: Assessment of water-induced soil erosion as a threat to Natura 2000 protected areas in Crete Island, Greece, *Sustainability-Basel*, 14, 2738, <https://doi.org/10.3390/su14052738>, 2022.
- Steppeler, J., G., D., Schättler, U., Bitzer, H. W., Gassmann, A., Damrath, U., and Gregoric, G.: Meso-gamma scale forecasts using the nonhydrostatic model LM, *Meteorol. Atmos. Phys.*, 82, 75–96, <https://doi.org/10.1007/s00703-001-0592-9>, 2003.
- Teng, H., Ma, Z., Chappell, A., Shi, Z., Liang, Z., and Yu, W.: Improving rainfall erosivity estimates using merged TRMM and gauge data, *Remote Sens.-Basel*, 9, 1134, <https://doi.org/10.3390/rs9111134>, 2017.
- Tramblay, Y., Neppel, L., Carreau, J., and Sanchez-Gomez, E.: Extreme value modelling of daily areal rainfall over Mediterranean catchments in a changing climate, *Hydrol. Process.*, 26, 3934–3944, 2012.
- Uber, M., Rössler, O., Astor, B., Hoffmann, T., Van Oost, K., and Hillebrand, G.: Climate change impacts on soil erosion and sediment delivery to German federal waterways: A case study of the Elbe basin, *Atmosphere-Basel*, 13, 1752, <https://doi.org/10.3390/atmos13111752>, 2022.
- Uber, M., Haller, M., Brendel, C., Hillebrand, G., and Hoffmann, T.: Past, present and future rainfall erosivity in Central Europe, version 1.0, Zenodo [data set], <https://doi.org/10.5281/zenodo.7628957>, 2023.
- Uppala, S. M., Källberg, P. W., Simmons, A. J., Andrae, U., Da Costa Bechtold, V., Fiorino, M., Gibson, J. K., Haseler, J., Hernandez, A., Kelly, G. A., Li, X., Onogi, K., Saarinen, S., Sokka, N., Allan, R. P., Andersson, E., Arpe, K., Balmaseda, M. A., Beljaars, A. C. M., Van De Berg, L., Bidlot, J., Bormann, N., Caires, S., Chevallier, F., Dethof, A., Dragosavac, M., Fisher, M., Fuentes, M., Hagemann, S., Hólm, E., Hoskins, B. J., Isaksen, L., Janssen, P. A. E. M., Jenne, R., McNally, A. P., Mahfouf, J.-F., Morcrette, J.-J., Rayner, N. A., Saunders, R. W., Simon, P., Sterl, A., Trenberth, K. E., Untch, A., Vasiljevic, D., Viterbo, P., and Woollen, J.: The ERA-40 re-analysis, *Q. J. Roy. Meteor. Soc.* 131, 2961–3012, <https://doi.org/10.1256/qj.04.176>, 2005.
- USDA Agricultural Research Service: User's reference guide. Revised Universal Soil Loss Equation version 2 (RUSLE2), Documentation, 444 pp., [https://www.ars.usda.gov/ARSUserFiles/60600505/RUSLE/RUSLE2\\_User\\_Ref\\_Guide.pdf](https://www.ars.usda.gov/ARSUserFiles/60600505/RUSLE/RUSLE2_User_Ref_Guide.pdf) (last access: 19 December 2023), 2008.
- Van Dijk, A., Bruijnzeel, L., and Rosewell, C.: Rainfall intensity–kinetic energy relationships: A critical literature appraisal, *J. Hydrol.*, 261, 1–23, [https://doi.org/10.1016/S0022-1694\(02\)00020-3](https://doi.org/10.1016/S0022-1694(02)00020-3), 2002.
- Verstraeten, G., Poesen, J., Demarée, G., and Salles, C.: Long-term (105 years) variability in rain erosivity as derived from 10 min rainfall depth data for Ukkel (Brussels, Belgium): Implications for assessing soil erosion rates, *J. Geophys. Res.-Atmos.*, 111, D22109, <https://doi.org/10.1029/2006JD007169>, 2006.
- Vrieling, A., Sterk, G., and de Jong, S. M.: Satellite-based estimation of rainfall erosivity for Africa, *J. Hydrol.*, 395, 235–241, <https://doi.org/10.1016/j.jhydrol.2010.10.035>, 2010.
- Wang, L., Cherkauer, K. A., and Flanagan, D. C.: Impacts of climate change on soil erosion in the Great Lakes region, *Water-SUI*, 10, 715, <https://doi.org/10.3390/w10060715>, 2018.
- Watanabe, M., Suzuki, T., O'ishi, R., Komuro, Y., Watanabe, S., Emori, S., Takemura, T., Chikira, M., Ogura, T., Sekiguchi, M., Takata, K., Yamazaki, D., Yokohata, T., Nozawa, T., Hasumi, H., Tatebe, H., and Kimoto, M.: Improved climate simulation by MIROC5: mean states, variability, and climate sensitivity, *J. Climate*, 23, 6312–6335, <https://doi.org/10.1175/2010JCLI3679.1>, 2010.
- Westra, S., Alexander, L. V., and Zwiers, F. W.: Global increasing trends in annual maximum daily precipitation, *J. Climate*, 26, 3904–3918, <https://doi.org/10.1029/2009JD012008>, 2013.
- Westra, S., Fowler, H. J., Evans, J. P., Alexander, L. V., Berg, P., Johnson, F., Kendon, E. J., Lenderink, G., and Roberts, N.: Future changes to the intensity and frequency of short-duration extreme rainfall, *Rev. Geophys.*, 52, 522–555, <https://doi.org/10.1002/2014RG000464>, 2014.
- Wilken, F., Baur, M., Sommer, M., Deumlich, D., Bens, O., and Fiener, P.: Uncertainties in rainfall kinetic energy-intensity relations for soil erosion modelling, *Catena*, 171, 234–244, <https://doi.org/10.1016/j.catena.2018.07.002>, 2018.
- Wischmeier, W. H.: A rainfall erosion index for a universal soil-loss equation, *Soil Sci. Soc. Am. J.*, 23, 246–249, 1959.
- Wischmeier, W. H. and Smith, D. D.: Rainfall energy and its relationship to soil loss, *EOS T. Am. Geophys. Un.*, 39, 285–291, <https://doi.org/10.1029/TR039i002p00285>, 1958.
- Wischmeier, W. H. and Smith, D. D.: Predicting rainfall erosion losses—a guide to conservation planning, United States Department of Agriculture, Agriculture Handbook No. 537, 58 pp., [https://books.google.de/books/about/Predicting\\_Rainfall\\_Erosion\\_Losses.html?id=rRAUAAAAYAAJ&redir\\_esc=y](https://books.google.de/books/about/Predicting_Rainfall_Erosion_Losses.html?id=rRAUAAAAYAAJ&redir_esc=y) (last access: 19 December 2023), 1978.
- Wisser, D., Frohking, S., Hagen, S., and Bierkens, M. F. P.: Beyond peak reservoir storage? A global estimate of declining water storage capacity in large reservoirs, *Water Resour. Res.*, 49, 5732–5739, <https://doi.org/10.1002/wrcr.20452>, 2013.
- Yin, S., Nearing, M., Borrelli, P., and Xue, X.: Rainfall erosivity: An overview of methodologies and applications, *Vadose Zone J.*, 16, 1–16, <https://doi.org/10.2136/vzj2017.06.0131>, 2017.
- Yue, T., Xie, Y., Yin, S., Yu, B., Miao, C., and Wang, W.: Effect of time resolution of rainfall measurements on the erosivity factor in the USLE in China, *International Soil and Water Conservation Research*, 8, 373–382, <https://doi.org/10.1016/j.iswcr.2020.06.001>, 2020.
- Zhao, G., Mu, X., Wen, Z., Wang, F., and Gao, P.: Soil erosion, conservation, and eco-environment changes in the Loess Plateau of China, *Land Degrad. Dev.*, 24, 499–510, <https://doi.org/10.1002/ldr.2246>, 2013.